

# Shaking table tests for the seismic stability of caisson type quaywalls both in ordinary 1g field and in centrifugal field

T.Inatomi, M.Kazama & Y.Murakami  
 Port and Harbour Research Institute, Yokosuka, Japan

**ABSTRACT:** A discussion of the seismic stability judgement of caisson type quaywalls by using shaking table tests data is presented. The shaking table tests are conducted both in ordinary 1g field and in centrifugal field. Dynamic external forces acting on the caisson structure such as  $M\ddot{X}$  (inertia force of caisson),  $P$  (dynamic earth pressure), and  $R$  (bottom friction force) are measured in the tests, and frequency dependant ratios  $P/M\ddot{X}$  and  $R/M\ddot{X}$  are specified. These tests results are compared with analysis by two degree of freedom system, and are reasonably explained. A new scheme to estimate the external forces used seismic stability judgement of the caisson type quaywalls is presented.

## 1 INTRODUCTION

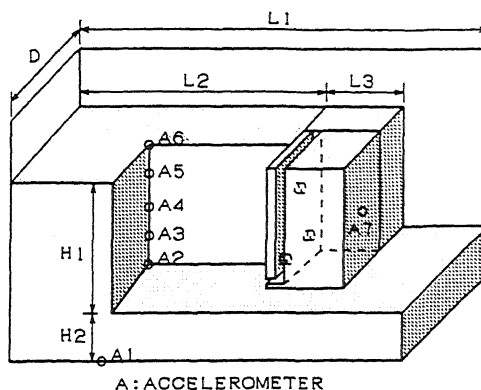
There are a lot of opportunities in recent years to construct port facilities in deep sea areas and the cost of construction is much higher than it was before. More rational and economical earthquake proof design procedures for these structures are required.

Seismic stability judgement of caisson type quaywalls has been one of the important engineering subjects. However, seismic earth pressure and inertia force acting on caisson during earthquake, that are used for seismic stability judgement, are estimated independently and are not enough reliable. The objectives of this paper are to study seismic stability of the caisson by shaking table tests, and to present a new scheme to estimate the external force for seismic stability judgement.

## 2 SHAKING TABLE TESTS

Shaking table tests were conducted both in ordinary 1G field and in centrifugal field. In 1G field test a 80cm high caisson model was used, on the other hand in centrifugal field test a 20cm high caisson model was used at a different centrifugal acceleration 4G, 30G and 40G. Fig.1 shows the view of caisson and backfill ground used in the tests. The dimensions of the prototype structure by a scaling law in centrifuge model test are shown in Table.1.

Table 2 shows physical properties of model ground such as a density and a shear wave velocity. The material of ground used in all



A: ACCELEROMETER  
 Fig.1 Model caisson and backfill ground.

Table 1 Model dimensions in prototype scale.

Test No.	ordinary 1G field		Centrifugal field		
	1	2	3	4	5
n (G)	1.0	1.0	4.05	31.9	40.5
H1(m)	0.8	0.8	0.8	6.4	8.1
H2(m)	0.2	0.2	0.2	1.7	2.4
L1(m)	3.0	3.0	2.4	19.1	24.3
L2(m)	2.0	2.0	1.7	11.9	15.1
L3(m)	0.48	0.48	0.5	4.0	5.1
D (m)	1.5	1.5	0.7	5.7	7.3

n : Vertical acceleration

H1-D: Length in prototype scale(see Fig.1)

test is dry Akita sand. Because of low confining pressure, in the less gravity field test, the model ground has the slower average shear wave velocity that is identified from the first natural frequency of the backfill ground.

Table 2 also shows input acceleration motion used here. In 1G field test several ten number of sinusoidal waves are used whose frequency is from 1Hz to 50Hz. In centrifugal test scaled earthquake motion is used whose frequency content is up to 300Hz.

Table 2 Physical properties of model ground and input motion.

Test No.	1	2	3	4	5
$\gamma_c$ (tf/m <sup>3</sup> )	1.574	1.090	1.332	1.332	1.524
$\gamma$ (tf/m <sup>3</sup> )	1.561	1.556	1.649	1.608	1.659
Dr (%)	53	52	78	66	81
$V_s$ (m/s)	108	108	175	245	260
Input Motion	sin wave 1Hz to 50Hz		earthquake motion Tokachi-oki 1968 at Hachinohe Port		
$A_{max}$ (Gal)	20	20	24	25	78
	50	50	41	57	212
	100	100	95	125	366
				152	389
				166	

$\gamma_c$  : Apparent unit weight of model caisson  
 $\gamma$  : Unit weight of the backfill ground  
 Dr : Relative density  
 $V_s$  : Shear wave velocity of ground  
 $A_{max}$  : Maximum acceleration in prototype scale

### 2.1 Test in ordinary 1G field

There are two kinds of test in ordinary 1G field. The difference in the tests is an unit weight of model caisson. The first natural frequency of backfill ground is about 27Hz. The model caisson with aluminium plates supported by three biaxial load cells enables us to measure directly the resultant force of dynamic earth pressure and of bottom friction force. The detail of how to measure the dynamic forces is given by Kazama(1989).

Fig.2 shows a coefficient of dynamic earth pressure with frequency of a 50Gal series test. Here we define dynamic earth pressure as the amplitude of a variation from a static earth pressure, and a coefficient  $K_{dy}$  is calculated by Equation (1).

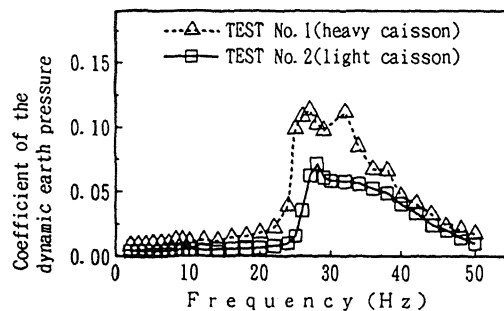


Fig.2 Coefficient of dynamic earth pressure with frequency. (1g field test 50Gal series)

$$K_{dy} = 2P / (\gamma H l^2) \quad (1)$$

Where  $P$  is the dynamic earth pressure amplitude modified into a value per unit depth. The dynamic earth pressure is amplified nearby the resonant frequency of backfill ground. It is also found that the dynamic earth pressure of a heavy model caisson is much larger than that of light one. This results can not be explained by usual earth pressure theory based on plastic equilibrium condition. The reason why is that the seismic earth pressure given by the theory does not depend on caisson weight. So, it is rational for estimating seismic stability to consider the dynamic behavior caused by interaction between caisson and backfill ground.

In general, for judgement of seismic stability the estimation of an external forces is the most important. When a steady state response to periodic load is imposed, an equilibrium of the external forces in horizontal direction can be written by the following form.

$$\{M\ddot{X} + P \cdot \exp(i\theta_1) + R \cdot \exp(i\theta_2)\} \cdot \exp(i\omega t) = 0 \quad (2)$$

Where notations are as follows:

- $M\ddot{X}$  : Amplitude of inertia force of caisson
- $P$  : Amplitude of dynamic earth pressure
- $R$  : Amplitude of bottom friction force
- $\theta_1$  : Phase difference between  $M\ddot{X}$  and  $P$
- $\theta_2$  : Phase difference between  $M\ddot{X}$  and  $R$
- $\omega$  : circular frequency of forced vibration
- $i$  :  $\sqrt{-1}$
- $t$  : time

A non-dimensional version of this equation is useful. In this case a dynamic system is represented by non-dimensional parameters ( $P/M\ddot{X}$ ), ( $R/M\ddot{X}$ ),  $\theta_1$  and  $\theta_2$ . With these non-dimensional factors the equation becomes

$$1 + (P/M\ddot{X})\exp(i\theta_1) + (R/M\ddot{X})\exp(i\theta_2) = 0 \quad (3)$$

Following this equation, we shall focus our attention on the non-dimensional factors of caisson and backfill ground system.

Fig.3 shows the phase difference  $\theta_1$  and  $\theta_2$  described above with frequency obtained by the experiment in 1G field. In low frequency range both  $\theta_1$  and  $\theta_2$  are about 180°. On the other hand in higher frequency range over the first natural frequency of backfill ground ( $f_{g1}$ ), i.e.  $f > 27\text{Hz}$ ,  $\theta_2$  approaches to 360°. It indicates that in lower frequency range than  $f_{g1}$ ,  $P$  and  $R$  resist  $M\ddot{X}$ , but in the higher frequency range than  $f_{g1}$ ,  $R$  and  $M\ddot{X}$  become to resist  $P$ .

Fig.4 shows the ratio ( $P/M\ddot{X}$ ) and ( $R/M\ddot{X}$ ) with frequency. The ratio ( $R/M\ddot{X}$ ) in low frequency range is about 0.7 (test No.1) and 0.8 (test No.2). In other words the additional dynamic force that make sliding for the caisson is about 70~80% of inertia force.

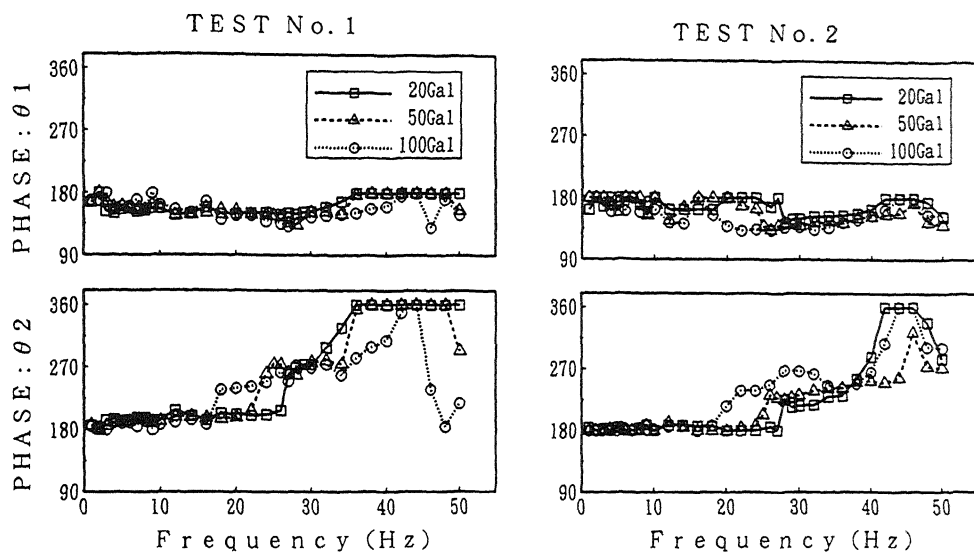


Fig.3 Phase difference  $\theta_1$  and  $\theta_2$  on 1G field test.

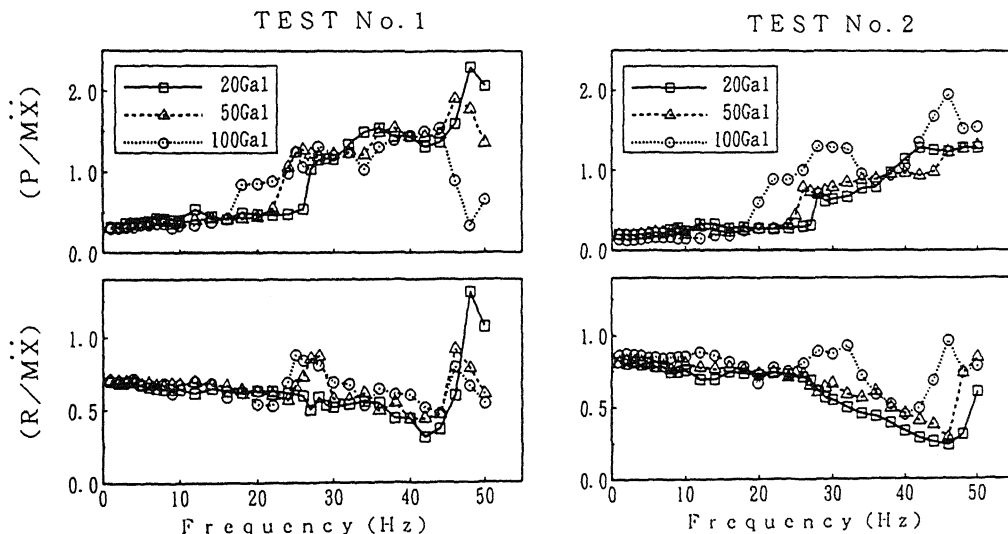


Fig.4 Ratio  $(P/M\ddot{X})$  and  $(R/M\ddot{X})$  on 1G field test.

## 2.2 Tests in centrifugal field

Centrifuge model test is known to satisfy the similitude for the models of geotechnical materials. We can consider the results of centrifuge test in prototype scale.

We performed the test in centrifugal field using a centrifuge at P.H.R.I.(Port and Harbour Res. Inst.). The configuration of the centrifuge and of shaking table facilities are shown in Terashi(1985) and Inatomi(1989).

Fig.5 shows time histories of the external forces acting on caisson at a 40G centrifugal field (test No.5) in prototype scale. Cross sections with force vector described in Fig.5 shows the equilibrium of external forces at the

same time in horizontal direction. It is found that the dynamic component of earth pressure is the force against inertia force of caisson.

The spectrum of  $(R/M\ddot{X})$  and  $(P/M\ddot{X})$  on the test No.5. is plotted for different input acceleration series in Fig.6. As the frequency of forced vibration increases, the ratio  $(P/M\ddot{X})$  is amplified, and the ratio  $(R/M\ddot{X})$  decreases as the same as those of 1G field test. But no remarkable variation of the ratios appears in the frequency range described. It is also found that the effects of the strength of ground acceleration, so called "non-linearity", on these ratios is not so large. However in lower frequency range than 100Hz the ratio  $(P/M\ddot{X})$  of small input acceleration is relatively

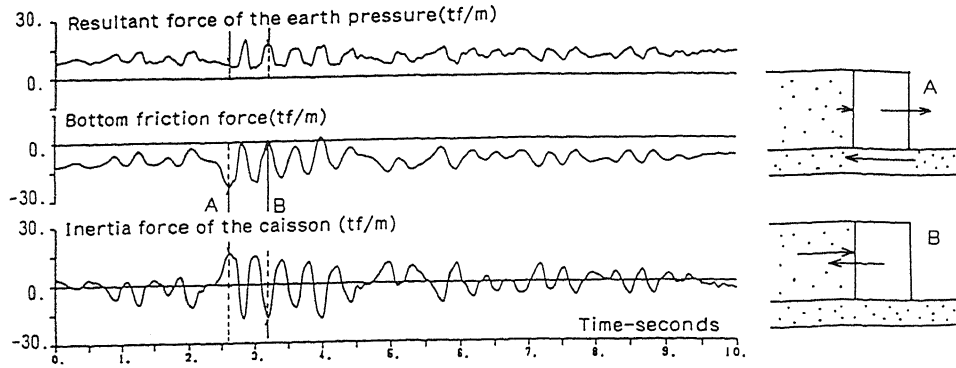


Fig.5 Time histories of the external forces acting on the caisson in test No.5 at a 212Gal stage.(Main portion including static component in prototype scale)

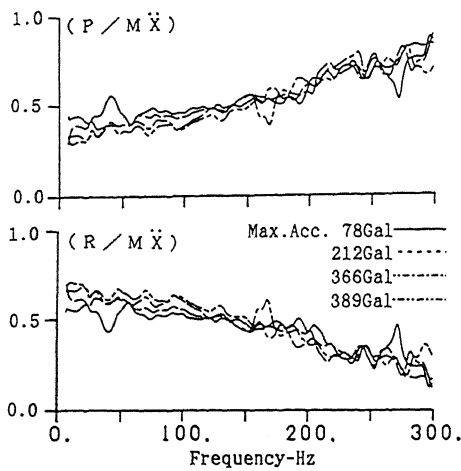


Fig.6 The ratio  $(R/M\ddot{X})$  and  $(P/M\ddot{X})$  with frequency at a 40G centrifugal field(test No.5).

larger compared with that in large input acceleration.

Fig.7 shows the comparison of the ratio  $(R/M\ddot{X})$  and  $(P/M\ddot{X})$  for different gravitational field. The ratio described in Fig.7 is the averaged value of different input acceleration series. The lateral axis is a non-dimensional frequency normalized by  $(V_s/4H_1)$ . The bottom friction force, that is the additional dynamic sliding force, is less than inertia force of caisson in all test. There is few difference between the results of test No.4(30G) and that of No.5(40G).

### 3 ANALYSIS BY TWO LUMPED MASSES SYSTEM

We simulate the results obtained from experiment considering the forced vibration of a system with two lumped masses as shown in Fig.8. The equation of motion of a system will be similar to Eq.(2) but with the addition of motion of ground.

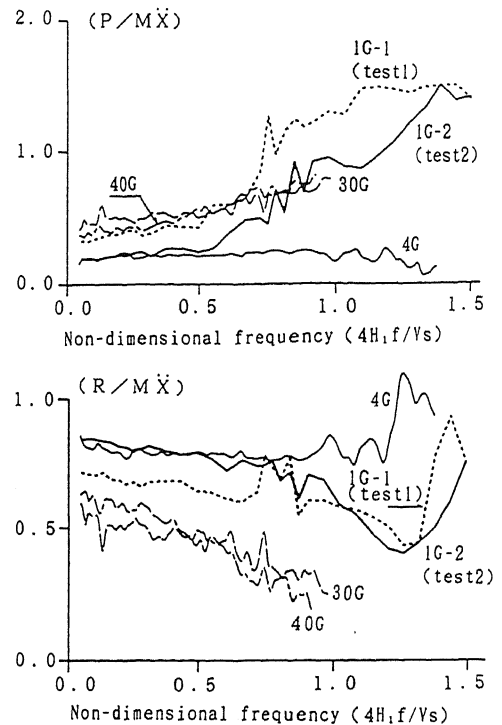


Fig.7 Comparison of the ratio  $(R/M\ddot{X})$  and  $(P/M\ddot{X})$  for different gravitational field test.

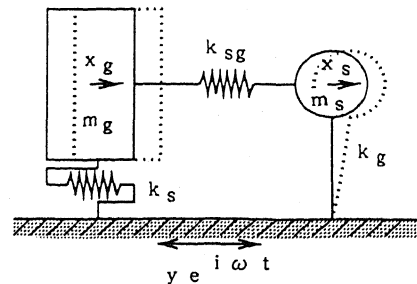


Fig.8 Two lumped masses system

Using the notation shown in Fig.8, we can write equation of motion for structure

$$-\frac{d^2(x_s+y)}{dt^2} + k_{sg}(x_g - x_s) - k_s x_s = 0 \quad (4a)$$

In this equation from 1st term to 3rd term corresponds to  $M\ddot{X}$ , P and R respectively as Eq.(2). It was assumed that dynamic earth pressure is directly proportional to relative displacement between structure and ground. For ground, equation of motion becomes

$$-\frac{d^2(x_g+y)}{dt^2} + k_{sg}(x_s - x_g) - k_g x_g = 0 \quad (4b)$$

The following notations will be introduced:

$\omega_s = \sqrt{k_s/m_s}$  : natural frequency of the structure itself  
 $\omega_g = \sqrt{k_g/m_g}$  : natural frequency of the ground itself  
 $\omega_{ss} = \sqrt{k_{sg}/m_s}$ ,  $\omega_{gg} = \sqrt{k_{sg}/m_g}$   
 $\omega_s/\omega_g = \alpha_s$ ,  $\omega_{ss}/\omega_g = \alpha_{ss}$ ,  $\omega_{gg}/\omega_g = \alpha_{gg}$

With these notations the steady state solution of system in frequency domain becomes

$$\begin{pmatrix} x_s \\ y \\ x_g \\ y \end{pmatrix} = \begin{bmatrix} (\frac{\omega}{\omega_g})^2 - \alpha_s^2 - \alpha_{ss}^2 & \alpha_{ss}^2 \\ \alpha_{gg}^2 & (\frac{\omega}{\omega_g})^2 - 1 - \alpha_{gg}^2 \end{bmatrix}^{-1} \begin{pmatrix} 1 \\ \frac{\omega}{\omega_g} \\ 1 \\ \frac{\omega}{\omega_g} \end{pmatrix} \quad (5)$$

$$(P/M\ddot{X}) = -\frac{\alpha_{ss}^2 \{(xg/y) - (xs/y)\}}{(\omega/\omega_g)^2 \{(xs/y) + 1\}} \quad (6)$$

$$(R/M\ddot{X}) = -\frac{\alpha_s^2 (xs/y)}{(\omega/\omega_g)^2 \{(xs/y) + 1\}} \quad (7)$$

It is clear that in case of  $\alpha_s = 1$  no dynamic earth pressure occur because of no intervention between response of structure and ground. A variation of the ratio  $(P/M\ddot{X})$  and  $(R/M\ddot{X})$  with non-dimensional frequency  $(\omega/\omega_g)$  is illustrated by plotting a graph of Eq.(5-7) as shown in Fig.9. Curves are drawn for different values of constant. Where we chose the frequency independent damping of

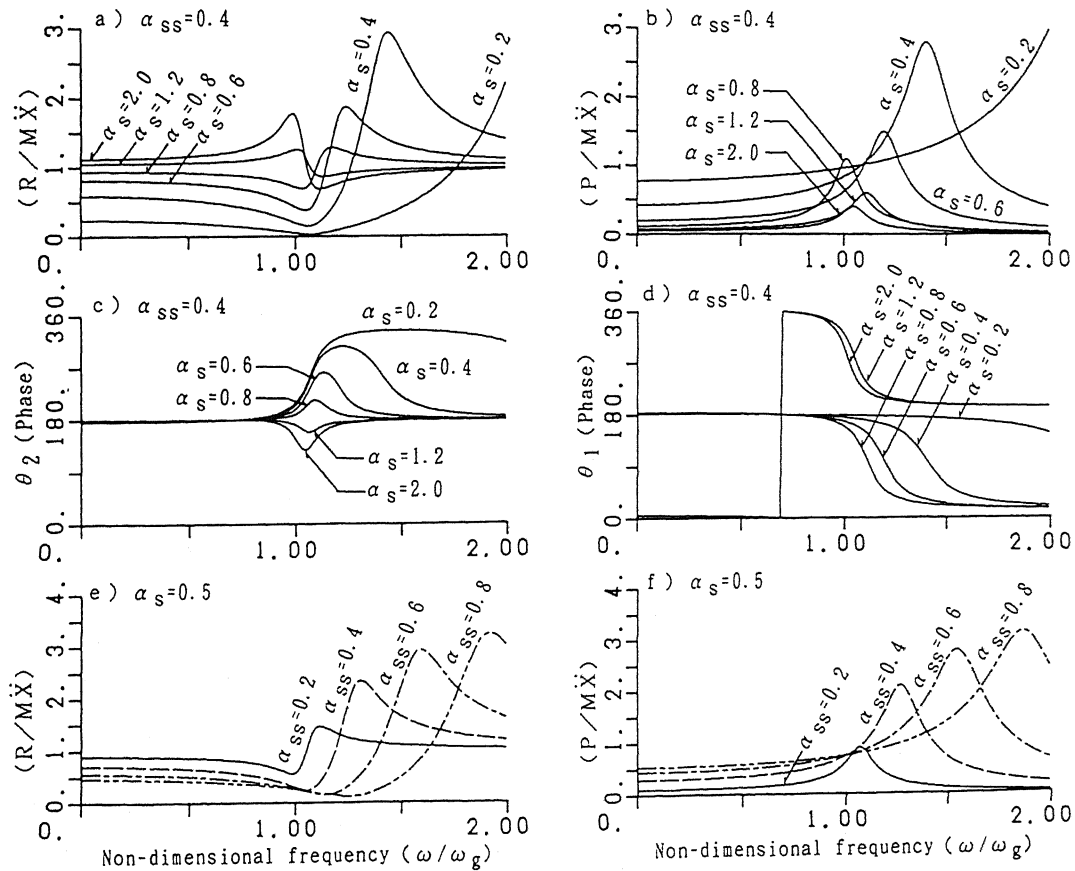


Fig.9 Variation of the non-dimensional factors  $(P/M\ddot{X})$ ,  $(R/M\ddot{X})$ ,  $\theta_1$  and  $\theta_2$  by the analysis with two lumped masses system. ( $\alpha_{gg} = 0.1$ )

spring  $k_g$ ,  $k_{sg}$  and  $k_s$  of 0.05, 0.10 and 0.05 respectively. From Fig.9 we find the following

1. In case of  $\alpha s < 1$ , the value of the ratio  $(R/M\ddot{X})$  is smaller than 1.0 and the phase difference  $\theta_1$  is about  $180^\circ$  in lower frequency range than  $\omega_g$ . As is seen in experimental results in Fig.7, there is the trend that  $(P/M\ddot{X})$  increase but  $(R/M\ddot{X})$  decrease with frequency

2. In case of  $\alpha s > 1$ , the value of the ratio  $(R/M\ddot{X})$  is larger than 1.0 and no phase difference of  $\theta_1$  appears in low frequency range.

3. From the nature written above,  $\omega s < \omega_g$  is consistent with the results of experiment, and a value of  $\alpha s$  seems to be about 0.4 ~ 0.8 comparing the value of  $(R/M\ddot{X})$  with that of experiment.

4. As the value of  $\alpha s$  increases, the ratio  $(R/M\ddot{X})$  decreases in relatively low frequency range compared with the natural frequency of ground itself ( $\omega_g$ ). That is harmonious with the results relation between test of No.1 and No.2, since  $\alpha s$  of test No.2 is larger than that of test No.1.

5. As values of  $\alpha s$  increase, the position of the peak occurs at higher frequency. Hence the values of  $\alpha s$  seem to be about 0.4, comparing the position of the peak with result of experiment.

#### 4 PRESENTATION OF NEW SCHEME TO ESTIMATE THE EXTERNAL FORCE

From an engineering point of view, we have to consider two type seismic earth pressures. One is used for the seismic stability of caisson structure. The other one is used for the design of structural members. In case of caisson stability judgement, we have to estimate the maximum bottom friction force during earthquake. On the other hand in case of structural design, we have to consider the seismic earth pressure strength and its distribution which cause maximum stress in structural members. Here we will pay our attention to only sliding stability of caisson.

Based on the model tests and the analyses presented here, the additional dynamic force to make caisson sliding depends on the dynamic behavior due to the interaction between caisson and backfill ground. From these studies, we will present the following new scheme for estimating the additional dynamic force.

1. In pseudostatic case  
When the frequency content of an earthquake motion is very low compared with the natural frequency of backfill ground, it is enough safe that we just consider the inertia force of caisson as an external force. For the low height caisson type quaywall with stiff backfill ground this method concludes economical.

2. In dynamic case  
When the frequency content of an earthquake

motion is close to the natural frequency range of backfill ground, the dynamic behavior becomes important.

If we will be able to define a design spectra of  $(R/M\ddot{X})$  with  $(\omega / \omega_g)$  under various conditions, we can easily obtain the additional dynamic sliding force due to earthquake, because estimating inertia force of caisson is easier than directly estimating dynamic earth pressure. This procedure is rational and probably economical compared with traditional procedure using seismic earth pressure.

In most practical case the second mode of backfill ground is negligible because the second natural frequency is usually very high compared with the predominant frequency of earthquake motion. Furthermore, a kinematic interaction effects becomes much larger in the frequency range dominating the second mode, that results in less response of a rigid structure. Therefore we just consider dynamic effects in the range of ground first natural frequency. Then the two lumped masses system described in the former division is useful for determine the design spectra.

#### 5 CONCLUSION

We obtained the fundamental information on the seismic stability of caisson type quaywall by the shaking table test under different gravitational field. Examples are the effects of caisson mass and of backfill ground resonance on dynamic earth pressure, the phase difference between dynamic earth pressure and inertia force of caisson, etc. Then we focused our attention on the ratio of dynamic earth pressure to inertia force, and of bottom friction force to inertia force, for understanding the dynamic behavior related to caisson dynamic stability. It was found that dynamic earth pressure was not a critical force to make caisson sliding in lower frequency range than the natural frequency of backfill ground. It could also be seen that tests results show the reasonable agreement with those by analysis with two lumped masses system. As a results of this study we presented a new economical scheme to estimate the external force for caisson seismic stability judgement.

#### REFERENCE

- Inatomi, T., Kazama, M., Noda, S. and Tsuchida, H. 1989. Centrifuge dynamic model test in PHRI, *Proc. of the 21th U.S./Japan panel on wind and seismic effects, U.S./Japan natural resource Conf.*
- Kazama, M. and Inatomi T. 1990. Model vibration test for the seismic earth pressure acting on the rigid caisson foundation, *Proc. of the JSCE, No.416/I-13 :419-428, (in Japanese).*
- Terashi, M. 1985. Development of PHRI geotechnical centrifuge and its application, *Report of the PHRI, Vol.24, No.3 :73-122.*